

# Modular Synthesis of Polybenzo[*b*]silole Compounds for Hole-Blocking Material in Phosphorescent Organic Light Emitting Diodes

Laurean Ilies,<sup>[a]</sup> Yoshiharu Sato,\*<sup>[b]</sup> Chikahiko Mitsui,<sup>[a]</sup> Hayato Tsuji,\*<sup>[a]</sup> and Eiichi Nakamura\*<sup>[a, b]</sup>

**Abstract:** A diversity-oriented synthetic strategy allowed us to design a series of conjugated molecules containing multiple benzosilole units that can be utilized as efficient hole-blocking materials for phosphorescent organic light emitting diodes (OLEDs). Some of these compounds showed a performance surpassing that of the current standard, bathocuproine. The new com-

pounds were easily synthesized in a modular fashion from a previously reported 3-stannyl benzosilole building unit. Studies on the properties of these

**Keywords:** benzosilole • hole-blocking material • materials science • phosphorescent OLED • synthesis design

compounds in solution and in the solid state indicate that they possess high electron affinity, high ionization potential, and form stable amorphous films that show high electron-drift mobility. The correlation between their molecular properties and the efficiency of the OLED device performance is also investigated.

## Introduction

Phosphorescent organic light emitting diodes (OLEDs)<sup>[1]</sup> can serve as highly efficient light emitting devices, because the phosphorescence emitters can harvest both the singlet and triplet excitons and achieve high performance of the device. This can be realized if the triplet excitons and positive charges (holes) can be confined into the emitting layer, and therefore exciton–exciton annihilation and charge recombination outside the active layer can be effectively avoided. Such confinement requires intercalation of an appropriate buffer layer between the emission layer and the electron-transporting layer. The buffer material, called a

hole-blocking material (HBM), must possess high triplet energy, high ionization potential, and low hole-drift mobility, so that it can block the diffusion of triplet excitons and of holes. Other requirements are high electron-drift mobility, formation of amorphous films, and thermal, chemical, and electrochemical stability. A widely used material as a HBM is bathocuproine (BCP),<sup>[2]</sup> which does not necessarily satisfy all of these requirements. Thus, we became interested in compounds bearing multiple 2,3-disubstituted benzo[*b*]silole units<sup>[3–5]</sup> (hereinafter benzosiloles) because of the high electron affinity of benzosilole<sup>[6]</sup> associated with its low-lying LUMO level<sup>[7]</sup> and the ready structural modification achievable by our diversity-oriented modular synthetic strategy.<sup>[8,9]</sup> We report herein a detailed study of the synthesis, properties, and application of polybenzosiloles as an efficient HBM for phosphorescent OLEDs. We also describe insights into the relationship between the device efficiency and the molecular properties.

## Results and Discussion

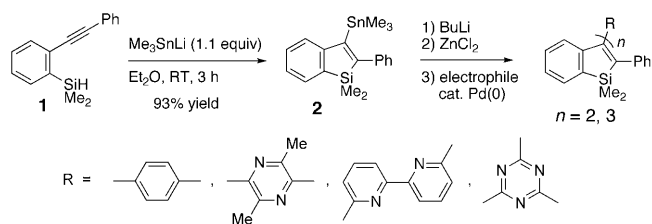
### Modular Synthesis of Functionalized Benzosiloles 3–6

For the synthesis of the polybenzosilole compounds, we relied on our modular strategy (Scheme 1).<sup>[3]</sup> Treatment of (2-alkynylphenyl)silane (**1**) with trimethylstannyl lithium in diethyl ether gave a stable 3-stannylbenzosilole (**2**) in excellent yield, which after transmetalation to a more reactive

[a] Dr. L. Ilies, C. Mitsui, Dr. H. Tsuji, Prof. Dr. E. Nakamura  
Department of Chemistry  
The University of Tokyo  
Hongo, Bunkyo-ku, Tokyo 113-0033 (Japan)  
Fax: (+81)3-5800-6889  
E-mail: nakamura@chem.s.u-tokyo.ac.jp  
tsuji@chem.s.u-tokyo.ac.jp

[b] Dr. Y. Sato, Prof. Dr. E. Nakamura  
Nakamura Functional Carbon Cluster Project, ERATO  
Japan Science and Technology Agency  
Hongo, Bunkyo-ku, Tokyo 113-0033 (Japan)  
E-mail: ysato@chem.s.u-tokyo.ac.jp

Supporting information for this article is available on the WWW under <http://dx.doi.org/10.1002/asia.201000112>.



Scheme 1. Modular synthesis of functionalized benzosiloles.

zinc intermediate was subjected to Pd<sup>0</sup>-catalyzed cross-coupling to achieve functionalization at the C-3 position.

The compounds thus prepared are illustrated in Table 1. Phenylene-linked benzosilole **3** was synthesized from 1,4-diiodobenzene in good yield (entry 1). Focusing on the ability of nitrogen-containing heterocycles to increase the electron affinity (EA),<sup>[10]</sup> we synthesized the pyrazine-core com-

Table 1. Preparation of conjugated molecules containing multiple benzosilole units.<sup>[a]</sup>

Entry	Electrophile	Product	Yield [%] <sup>[b]</sup>
1			84
2			96
3			64
4			71

[a] For the reaction conditions, see Scheme 1 and the Experimental Part. [b] Yield of isolated product.

#### Abstract in Japanese:

リン光 EL 素子は高い EL 発光効率を示す発光素子として注目を集めている。我々は 3-スタンニルベンゾシロールを合成モジュールとしてポリベンゾシロール正孔阻止材料を合成、機能評価したところ、ピラジン骨格を中心部に持つ化合物が、既存の材料バソクプロインよりも優れた素子性能を与えることを見出した。これら材料の電子親和力、イオン化ポテンシャル、電子移動度等、諸物性と EL 素子性能との関係についても考察した。

pound **4** in excellent yield by the coupling of **2** with dichloropyrazine (entry 2). This compound consists of two rotational isomers of **4** (NMR) because the methyl substituents on the pyrazine linker hamper the rotation of the benzosilole moieties.<sup>[11]</sup> In light of the popularity of the bipyridyl motif for the design of *n*-type organic semiconductors,<sup>[12]</sup> we prepared the bipyridyl-core compound **5** in good yield by the coupling of **2** with dibromobipyridyl (entry 3). Triple coupling of **2** with 2,4,6-trichlorotriazine (cyanuric chloride) proceeded smoothly, and the triazine-linked<sup>[13]</sup> benzosilole **6** was obtained in good yield (entry 4).

#### Properties

Studies on compounds **3–6** in solution and in the solid state (Tables 2 and 3) showed that these compounds possess high EA and IP, and form stable amorphous films showing high electron-drift mobility.

As shown in Table 2, the absorption maxima of compounds **3–6** were in the range of 288–325 nm, with an optical gap of 3.10–3.26 eV, which is rather small because of the limited conjugation in these nonplanar compounds. The fluorescence maximum of phenylene-linked compound **3** was approximately 390 nm, while introduction of nitrogen heterocycles in **4–6** red-shifted the emission to 460 nm. These 2,3-disubstituted benzosiloles showed very low emission quantum yields in solution, as expected from previous reports on polysubstituted siloles.<sup>[14]</sup> All compounds showed irreversible reduction waves in THF at a scan rate of 100 mV s<sup>-1</sup>, the first reduction potential being in the range of -2.21 to -2.62 V versus a ferrocene standard. The introduction of nitrogen-containing heterocycles caused an increase in the electron affinity of the compounds, but this effect was

rather small, probably because of the nonplanarity of the compounds (Figure 1). The triazine-linked **6**, however, exhibited a significantly higher reduction potential (entry 6), probably because of the high electron affinity of the triazine unit.<sup>[13]</sup>

Compounds **3–6** form stable amorphous films possessing high electron-drift mobility (Table 3). Fast cooling of a melt of compounds **3–6** gave an amorphous solid, and its thermal behavior was evaluated by differential scanning calorimetry (DSC). The stability of the amorphous state increases as the

Table 2. Optical and electrochemical properties in solution for compounds 3–6.

Cmpd.	$\lambda_{\text{abs}}^{[a]}$ [nm]	Optical gap [eV]	$\lambda_{\text{em}}^{[a,b]}$ [nm]	$\Phi_{\text{F}}^{[c]}$	$E_{\text{redn}}^{[d]}$ [V]	IP <sup>[e]</sup> [eV]	EA <sup>[f]</sup> [eV]
3	325	3.26	392	0.02	-2.62	5.44	2.18
4	296	3.26	462	0.01	-2.50	5.56	2.30
5	322	3.26	460	0.01	-2.57	5.49	2.23
6	288	3.10	–	<0.01	-2.21	5.69	2.59

[a] In dichloromethane. [b] Irradiated at 320–340 nm. [c] Quinine sulfate in aqueous 0.5 M sulfuric acid was used as a reference. [d] First reduction potential determined by CV for a THF solution (0.5 mmol L<sup>-1</sup>), using TBAP (0.1 mol L<sup>-1</sup>) as an electrolyte. The scan rate was 100 mV s<sup>-1</sup>, three cycles per measurement. Glassy carbon was used as the working electrode, platinum wire as the counter electrode and Ag<sup>+</sup>/Ag as a standard electrode.  $E_{\text{redn}}$  refers to the cathode potential for the irreversible reduction wave, and its value was determined by DPV and corrected from a ferrocene standard. [e] Inferred from the optical gap and EA. [f] EA = 4.8 +  $E_{\text{redn}}$ .

Table 3. Solid-state properties and triplet energy for compounds 3–6.

Cmpd.	$T_{\text{g}}^{[a]}$ [°C]	$T_{\text{c}}^{[a]}$ [°C]	$T_{\text{m}}^{[a]}$ [°C]	$\mu_{\text{e}}^{[b]}$ [cm <sup>2</sup> V s]	$E_{\text{T}}^{[c]}$ [eV]
3	66	125	234	$6 \times 10^{-4}$	2.38
4	83	138	225	$7 \times 10^{-4}$	2.43
5	103	148	300	$2 \times 10^{-3}$	2.39
6	112	149	261	$7 \times 10^{-6}$	2.32

[a] Determined by differential scanning calorimetry.  $T_{\text{g}}$ ,  $T_{\text{c}}$ , and  $T_{\text{m}}$  refer to the glass transition temperature, crystallization temperature and melting temperature, respectively. [b] Electron-drift mobility for a thick amorphous film, determined by the time-of-flight technique, at an applied electric field of  $5 \times 10^5$  V cm<sup>-1</sup>. [c] The triplet energy level was estimated by a TD-DFT calculation.

molecular size increased, and tris-benzosilole 6 showed a glass transition temperature as high as 112 °C. The electron-drift mobility of a thick film of compounds 3–6 was measured by the time-of-flight technique.<sup>[15]</sup> Except for the poorly conducting triazine-linked 6, all benzosiloles showed high electron-drift mobility in the  $10^{-4}$ – $10^{-3}$  cm<sup>2</sup> V s range, at an applied electric field of  $5 \times 10^5$  V cm<sup>-1</sup>. The bipyridyl-linked 5 showed the highest value in the series, probably because of a synergetic effect between the benzosilole unit and the bipyridyl moiety.<sup>[12]</sup> The triazine-linked 6 showed low

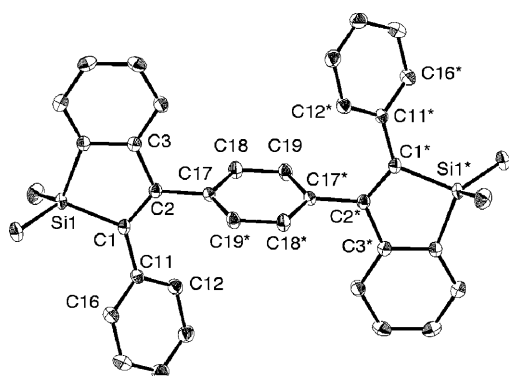


Figure 1. ORTEP drawing of phenylene-linked benzosilole 3 (50% probability for thermal ellipsoids). Hydrogen atoms are omitted for clarity. Selected bond angles: Si1–C1–C2–C3 = -6.73(14)°; Si1–C1–C11–C12 = 44.41(17)°; C1–C2–C17–C19 = 72.25(19)°.

electron mobility, presumably because of the excessively high electron affinity of the triazine moiety.<sup>[13]</sup> The triplet energy was calculated by TD-DFT, and was found to depend by a small degree on the nature of the linker.

Single crystals of phenylene-linked benzosilole 3 suitable for crystallographic analysis were obtained by recrystallization from hexane/chloroform, the X-ray crystal structure being shown in Figure 1. While the benzosilole framework is planar, the 2-substituent is tilted out of the benzosilole plane at a dihedral angle of 44.41(17)°. The similar dihedral angles reported by Yamaguchi for 1,4-bis(1,1-dimethylbenzosilol-2-yl)benzene are smaller (average 27°),<sup>[5d]</sup> suggesting that the 3-substituent in 3 forces the 2-substituent out of the benzosilole plane. The 3-substituent is also tilted out at 72.25(19)°, explaining the small effect of this substituent on the LUMO level of the molecule (Table 2). The crystal packing of 3 (Figure 2) suggests the lack of strong intermolecular interactions, explaining the facile formation of the amorphous state.

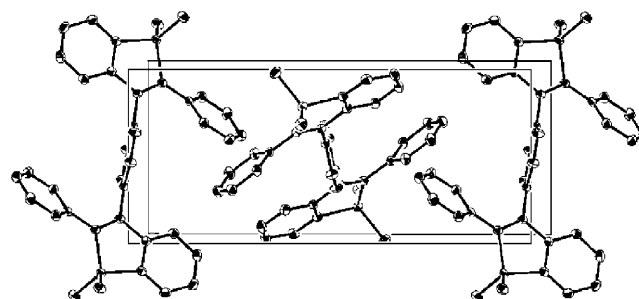


Figure 2. The crystal packing of phenylene-linked benzosilole 3.

### The Use of Benzosiloles as HBM for Phosphorescent OLEDs

Next, we investigated the behavior of benzosiloles 3–6 as HBM for phosphorescent OLEDs. The devices were fabricated employing the standard materials<sup>[11]</sup> (Figure 3): transparent glass coated with indium-tin oxide (ITO) was used as an anode, poly(ethylenedioxy)thiophene:polystyrene sulfonate (PEDOT:PSS, 30 nm) was used as a hole-injection material, *N,N'*-di-[(1-naphthyl)-*N,N'*-diphenyl]-1,1'-biphenyl-4,4'-diamine ( $\alpha$ -NPD, 45 nm) was used as a hole-transporting material, ambipolar 4,4'-bis(carbazol-9-yl)biphenyl (CBP, 30 nm) doped with 4 wt % green phosphorescent *fac*-Ir(ppy)<sub>3</sub> was used as an emission layer, benzosilole 3–6 or BCP (10 nm) was used as a HBM, tris(8-hydroxyquinolato)aluminum (Alq<sub>3</sub>, 20 nm) was used as an electron-transporting material, and aluminum (80 nm) coated with 8-hydroxyquinolinato lithium (Liq, 1 nm) was used as a cathode.

The characteristics of the device are summarized in Figures 4 and 5 and Table 4. Compounds 3–5 showed an overall performance comparable with that of BCP, and the pyrazine-linked compound 4 showed the highest performance, surpassing BCP for the driving voltage, luminance efficiency, current efficiency, and maximum luminance (Table 4). The

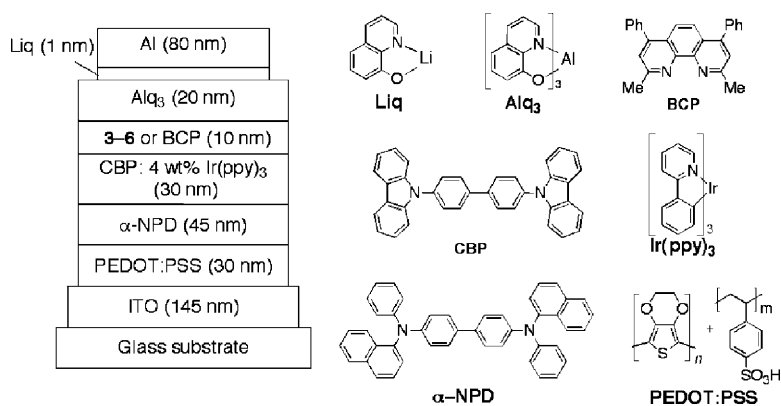


Figure 3. The structure of phosphorescent OLED and the materials utilized.

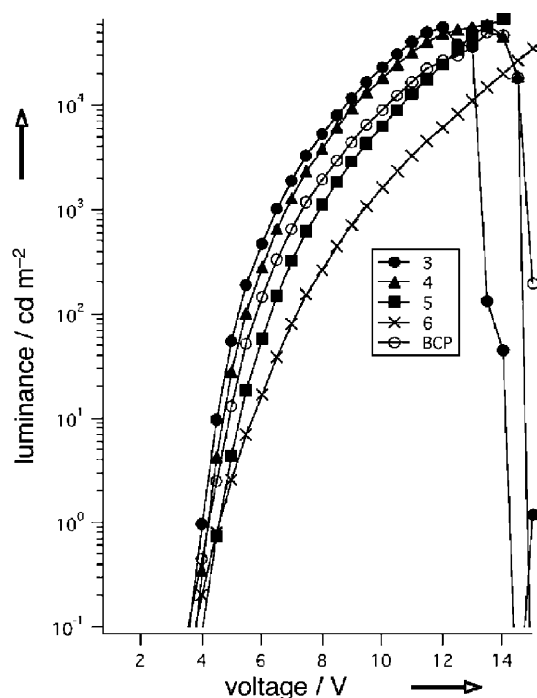


Figure 4. L-V characteristics of a phosphorescent OLED utilizing benzo-silole 3-6 or BCP as a HBM.

device using triazine-linked compound **6** showed a lower performance.

To gain insight into the factors controlling the efficiency of HBMs, we plotted the external quantum efficiency (EQE) recorded at a luminance of  $1000 \text{ cd m}^{-2}$  versus EA (Figure 6), IP (Figure 7),  $E_T$  (Figure 8), and electron mobility ( $\mu_e$ ) (Figure 9). As shown in Figure 9, for compounds **3-5**, which possess electron-drift mobility higher than  $\text{Alq}_3$  ( $\sim 1 \times 10^{-5} \text{ cm}^2 \text{ V s}$ ),<sup>[16]</sup> factors other than the mobility control their performance. However, the poorly semiconducting **6**, which possesses a lower electron-drift mobility than  $\text{Alq}_3$ , showed poor performance, regardless of its other properties. The performance of the high mobility compounds **3-5** showed almost linear dependence on their EA, IP, and  $E_T$ . We assume that higher EA favors injection of electrons from

the aluminium cathode, while higher IP and  $E_T$  efficiently confine the holes, and the triplet excitons, respectively, into the emission layer. These correlations suggest that for a series of structurally related compounds, rational design of efficient HBMs could be achieved by evaluating their molecular properties.

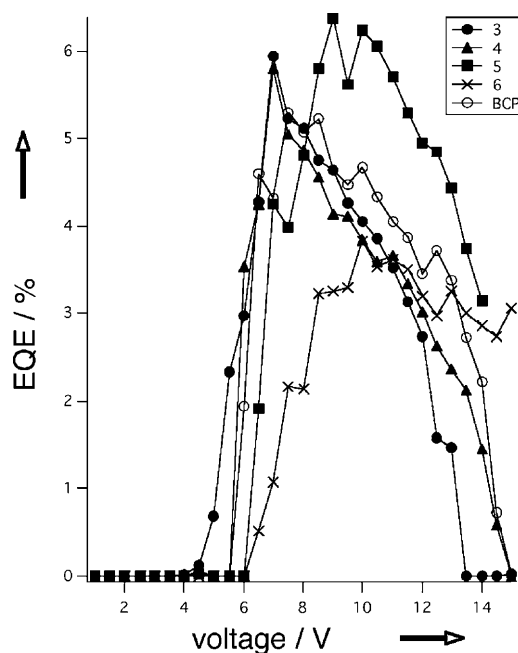


Figure 5. EQE characteristics of a phosphorescent OLED utilizing benzo-silole 3-6 or BCP as a HBM.

Table 4. Summary of the characteristics of a green phosphorescence OLED utilizing compounds 3-6 or BCP as HBM.<sup>[a]</sup>

HBM	$V_{1000}$ <sup>[b]</sup> [V]	$\eta_{1000}$ <sup>[c]</sup> [lm/W]	$L/J_{1000}$ <sup>[d]</sup> [cd A] <sup>-1</sup>	$\text{EQE}_{1000}$ <sup>[e]</sup> [%]	$L_{\text{max}}$ <sup>[f]</sup> [cd m <sup>-2</sup> ]
<b>3</b>	6.5	6.5	13.5	4.3	55 530
<b>4</b>	6.9	7.6	17.0	5.8	59 400
<b>5</b>	7.9	5.7	14.6	4.8	66 690
<b>6</b>	9.5	2.9	8.7	3.3	34 950
BCP	7.4	6.5	15.5	5.2	49 940

[a] All OLED performance data were collected at a luminance of  $1000 \text{ cd m}^{-2}$ . [b] Driving voltage. [c] Luminance efficiency. [d] Current efficiency. [e] External quantum efficiency. [f] Maximum luminance.

## Conclusions

A series of conjugated molecules containing multiple benzo-silole units linked by an aromatic core have been synthesized. They showed high electron affinity and readily

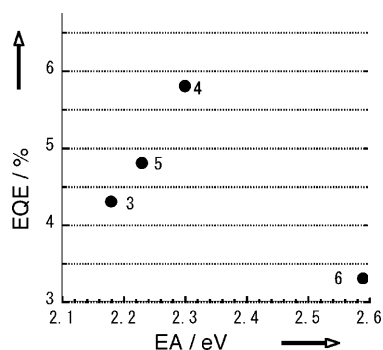


Figure 6. Correlation of EQE with EA.

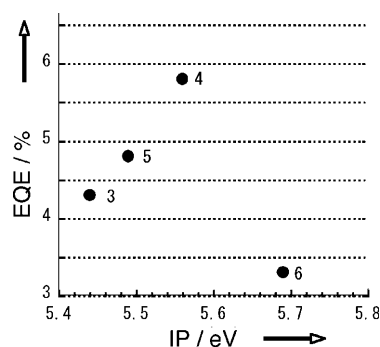


Figure 7. Correlation of EQE with IP.

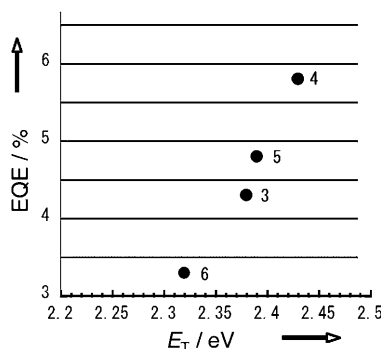


Figure 8. Correlation of EQE with  $E_T$ .

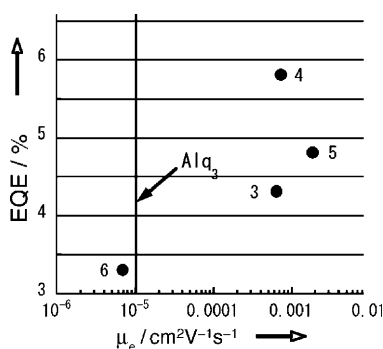


Figure 9. Correlation of EQE with the electron-drift mobility, and comparison with the electron-drift mobility of Alq<sub>3</sub>.

formed stable amorphous films that possess a high electron-drift mobility. The functionalized benzosiloles were then utilized as HBMs for phosphorescent OLEDs, and they exhibited a good overall performance that surpasses the current standard material, BCP. Correlation of the device efficiency with the molecular properties of the benzosiloles suggested that for the HBM materials that possess higher electron-drift mobility than the electron-transporting material (e.g., Alq<sub>3</sub>), the device performance increases almost linearly with the electron affinity, the ionization potential, and the triplet energy of the HBM.

## Experimental Section

Compounds **3–6** were prepared according to our previously reported procedure.<sup>[3]</sup>

Data for the new compounds:

**2,5-Bis(1,1-dimethyl-2-phenylbenzo[*b*]silol-3-yl)-3,6-dimethylpyrazine (4):** white solid. M.p.: 224–225 °C; <sup>1</sup>H NMR (500 MHz, C<sub>2</sub>D<sub>2</sub>Cl<sub>4</sub>): two isomers, ~6:1 ratio.  $\delta$  = 0.40+0.41 (s, 6H, Si(CH<sub>3</sub>)<sub>2</sub>), 0.65+0.66 (d, 6H, Si(CH<sub>3</sub>)<sub>2</sub>), 2.15+2.16 (s, 6H, PyrazineCH<sub>3</sub>), 6.62–6.81 (m, 2H), 7.00–7.06 (m, 4H), 7.18–7.30 (m, 10H), 7.64–7.66 ppm (m, 2H). <sup>13</sup>C NMR (125 MHz, CD<sub>2</sub>Cl<sub>2</sub>): mixture of two isomers.  $\delta$  = -4.2, -2.6, 21.15, 21.24, 123.7, 123.9, 126.9, 127.0, 127.37, 127.39, 128.2, 128.4, 128.6, 128.8, 130.2, 132.2, 138.3, 139.8, 145.7, 149.3, 149.4, 149.6, 149.9, 150.2 ppm. TOF MS (APCI+): 577 [M+1]; elemental analysis: calcd (%) for C<sub>38</sub>H<sub>36</sub>N<sub>2</sub>Si<sub>2</sub>: C 79.12, H 6.29, N 4.86; found: C 78.84, H 6.33, N 4.57.

**6,6'-Bis(1,1-dimethyl-2-phenylbenzo[*b*]silol-3-yl)-2,2'-bipyridine (5):** white solid. M.p.: 294–295 °C. <sup>1</sup>H NMR (500 MHz, C<sub>2</sub>D<sub>2</sub>Cl<sub>4</sub>):  $\delta$  = 0.52 (s, 12H, Si(CH<sub>3</sub>)<sub>2</sub>), 7.04–7.37 (m, 18H), 7.68 (d, *J* = 8.0 Hz, 4H), 8.07 ppm (d, *J* = 8.0 Hz, 2H); <sup>13</sup>C NMR (100 MHz, C<sub>2</sub>D<sub>2</sub>Cl<sub>4</sub>, 70 °C):  $\delta$  = -3.4, 120.0, 124.4, 125.4, 126.0, 126.8, 128.2, 128.5, 129.8, 131.8, 136.9, 138.4, 140.0, 145.5, 149.9, 151.8, 156.4, 156.7 ppm; TOF MS (APCI+): 625 [M+1]; elemental analysis: calcd (%) for C<sub>42</sub>H<sub>36</sub>N<sub>2</sub>Si<sub>2</sub>: C 80.72, H 5.81, N 4.48; found: C 80.66, H 5.83, N 4.44.

**1,3,5-tris(1,1-dimethyl-2-phenylbenzosilol-3-yl)triazine (6):** white solid. M.p.: 256–257 °C; <sup>1</sup>H NMR (500 MHz, CDCl<sub>3</sub>):  $\delta$  = 0.38 (s, 18H, Si(CH<sub>3</sub>)<sub>2</sub>), 6.26 (d, *J* = 7.5 Hz, 3H), 6.94–6.96 (m, 6H), 7.07–7.10 (m, 3H), 7.18 (t, *J* = 7.0 Hz, 3H), 7.20–7.24 (m, 9H), 7.51 ppm (d, *J* = 7.0 Hz, 3H); <sup>13</sup>C NMR (125 MHz, CDCl<sub>3</sub>):  $\delta$  = -4.1, 123.1, 126.3, 126.8, 128.0, 128.4, 130.1, 131.7, 137.5, 139.1, 147.98, 148.0, 148.6, 174.9 ppm; TOF MS (APCI+): 784 [M+1]; elemental analysis: calcd (%) for C<sub>51</sub>H<sub>45</sub>N<sub>3</sub>Si<sub>3</sub>: C 78.11, H 5.78, N 5.36; found: C 77.94, H 5.93, N 5.25.

UV/Vis absorption spectra were recorded with a JASCO V-570 spectrometer at a resolution of 0.5 nm. Spectroscopy-grade dichloromethane was used as the solvent. Ca. 10<sup>-5</sup> mol L<sup>-1</sup> sample solutions in a 1 cm square quartz cell were used for the measurements. All measurements were performed at room temperature.

Fluorescence spectra were recorded with a HITACHI F-4500 spectrometer. Degassed spectroscopy-grade dichloromethane was used as the solvent. Quantum yields were determined by comparison with the quantum yield (0.546) of a ca. 10<sup>-5</sup> mol L<sup>-1</sup> solution of quinine sulfate in 0.5 M sulfuric acid. The excitation was performed at 320–340 nm, on the flat region of the absorption spectrum. All measurements were performed at room temperature.

Cyclic voltammetry was performed using a HOKUTO DENKO HZ-5000 voltammetric analyzer. A glassy carbon electrode was used as the working electrode, a platinum coil as the counter electrode and Ag<sup>+</sup>/Ag as the reference electrode, at a scan rate of 100 mV s<sup>-1</sup>, three cycles per measurement. The compounds were dissolved in degassed, dry THF at a concentration of ca. 5 × 10<sup>-3</sup> mol L<sup>-1</sup>, and tetrabutylammonium perchlorate at a concentration of 0.1 mol L<sup>-1</sup> was added as an electrolyte. The reduction potentials were determined by differential pulse voltammetry (DPV), and were corrected from a ferrocene standard.

The single crystal X-ray diffraction study was carried out on a Rigaku MERCURY CCD system. Single crystals were obtained by slowly cooling a solution of **3** in hexane/chloroform (9:1).

Differential scanning calorimetry was performed on a NETZSCH thermal analyzer (DSC 204/F1). An amorphous sample was obtained by fast cooling of the melt of benzosiloles **3–6**, and the obtained sample was heated at a rate of 10 K min<sup>-1</sup> under N<sub>2</sub> gas, at a flow rate of 18 mL min<sup>-1</sup>.

The time-of-flight measurements were performed at Sumitomo Heavy Industries Advanced Machinery, TOF-401. Films were deposited on ITO-coated (145 nm) glass substrates. The vacuum deposition was performed at ULVAC KIKO (VPC-260). The films were deposited by vacuum sublimation at 1 × 10<sup>-3</sup> Pa, with an average deposition rate of 20–30 nm s<sup>-1</sup>. The ITO-coated glass substrate was spaced at 100 mm from the sample and was kept at 25 °C. The thickness of the films obtained was 3–5 μm. All calculations were performed using the Gaussian 03 program.<sup>[17]</sup> The geometries of benzosiloles were optimized at the B3LYP/6-31G\* level. The triplet energy levels were determined by TD-DFT calculations at the B3LYP/6-31G\* level, utilizing the optimized geometries.

For the device fabrication and evaluation, compounds **3–6** of analytical purity were further purified by train sublimation. All of the other materials were commercially available and were used as purchased. An ITO-coated glass substrate treated by O<sub>3</sub>-plasma was used as the anode. A PEDOT:PSS water dispersion was spin-coated into this substrate, it was dried at 120 °C, then it was annealed at 180 °C under nitrogen. All layers were sequentially vacuum deposited into this substrate at a pressure of 2 × 10<sup>-4</sup> Pa or less. Finally, the device was sealed by encapsulation with fresh desiccant under nitrogen. The emissive area of the device was 2 × 2 mm<sup>2</sup>.

Device structure: glass/ITO (145 nm)/PEDOT:PSS (30 nm)/α-NPD (45 nm)/CBP:Ir(ppy)<sub>3</sub> (4 wt %) (30 nm)/**3–6** or BCP (10 nm)/Alq<sub>3</sub> (20 nm)/Liq (1 nm)/Al (80 nm).

## Acknowledgements

We thank MEXT (KAKENHI for E.N., No. 18105004 and for H.T., No. 20685005) and the Global COE Program for Chemistry Innovation. L.I. and C.M. thank the Research Fellowship of the Japan Society for the Promotion of Science for Young Scientists (No. 19-10183 and 21-9262, respectively).

- 1) a) *Organic Light-Emitting Devices. Synthesis Properties and Applications* (Eds.: K. Müllen, U. Scherf), Wiley-VCH, Weinheim, **2006**; b) *Organic Light-Emitting Devices. A Survey* (Ed.: J. Shinar), Springer, New York, **2004**; c) *Organic Light-Emitting Materials and Devices* (Eds.: Z. Li, H. Meng), CRC Press, Boca Raton, **2007**; d) *Highly Efficient OLEDs with Phosphorescent Materials* (Ed.: H. Yersin), Wiley-VCH, Weinheim, **2008**.
- 2) D. F. O'Brien, M. A. Baldo, M. E. Thompson, S. R. Forrest, *Appl. Phys. Lett.* **1999**, *75*, 442–444.
- 3) L. Ilies, H. Tsuji, Y. Sato, E. Nakamura, *J. Am. Chem. Soc.* **2008**, *130*, 4240–4241.
- 4) J. Dubac, A. Laporterie, G. Manuel, *Chem. Rev.* **1990**, *90*, 215–263 and references therein.
- 5) Selected recent examples: a) G. Märkl, H. K. P. Berr, *Tetrahedron Lett.* **1992**, *33*, 1601–1604; b) A. Kunai, Y. Yuzuriha, A. Naka, M. Ishikawa, *J. Organomet. Chem.* **1993**, *455*, 77–81; c) T. Sudo, N. Asao, Y. Yamamoto, *J. Org. Chem.* **2000**, *65*, 8919–8923; d) C. Xu, A. Wakamiya, S. Yamaguchi, *Org. Lett.* **2004**, *6*, 3707–3710; e) T. Matsuda, S. Kadowaki, Y. Yamaguchi, M. Murakami, *Chem. Commun.* **2008**, 2744–2746; f) T. Matsuda, Y. Yamaguchi, M. Murakami, *Synlett* **2008**, 561–564; g) M. Tobisu, M. Onoe, Y. Kita, N. Chatani, *J. Am. Chem. Soc.* **2009**, *131*, 7506–7507; h) L. Ilies, H. Tsuji, E. Nakamura, *Org. Lett.* **2009**, *11*, 3966–3968.
- 6) a) Y. Shirota, H. Kageyama, *Chem. Rev.* **2007**, *107*, 953–1010; b) A. P. Kulkarni, C. J. Tonzola, A. Babel, S. A. Jenekhe, *Chem. Mater.* **2004**, *16*, 4556–4573.
- 7) a) U. Salzner, J. B. Lagowski, P. G. Pickup, R. A. Poirier, *Synth. Met.* **1998**, *96*, 177–189; b) K. Tamao, M. Uchida, T. Izumizawa, K. Furukawa, S. Yamaguchi, *J. Am. Chem. Soc.* **1996**, *118*, 11974–11975; c) H. Murata, G. G. Malliaras, M. Uchida, Y. Shen, Z. H. Kafafi, *Chem. Phys. Lett.* **2001**, *339*, 161–166.
- 8) a) M. Nakamura, L. Ilies, S. Otsubo, E. Nakamura, *Angew. Chem.* **2006**, *118*, 958–961; *Angew. Chem. Int. Ed.* **2006**, *45*, 944–947; b) M. Nakamura, L. Ilies, S. Otsubo, E. Nakamura, *Org. Lett.* **2006**, *8*, 2803–2805; c) H. Tsuji, K. Sato, L. Ilies, Y. Itoh, Y. Sato, E. Nakamura, *Org. Lett.* **2008**, *10*, 2263–2265; d) X. Zhu, C. Mitsui, H. Tsuji, E. Nakamura, *J. Am. Chem. Soc.* **2009**, *131*, 13596–13597.
- 9) a) H. Tsuji, C. Mitsui, L. Ilies, Y. Sato, E. Nakamura, *J. Am. Chem. Soc.* **2007**, *129*, 11902–11903; b) H. Tsuji, Y. Yokoi, C. Mitsui, L. Ilies, Y. Sato, E. Nakamura, *Chem. Asian J.* **2009**, *4*, 655–657; c) H. Tsuji, K. Sato, Y. Sato, E. Nakamura, *J. Mater. Chem.* **2009**, *19*, 3364–3366; d) H. Tsuji, C. Mitsui, Y. Sato, E. Nakamura, *Adv. Mater.* **2009**, *21*, 3776–3779.
- 10) For example: M. Uchida, T. Izumizawa, T. Nakano, S. Yamaguchi, K. Tamao, K. Furukawa, *Chem. Mater.* **2001**, *13*, 2680–2680.
- 11) For utilization of stereogenic centers in a molecule to stabilize the amorphous state, see reference [8c].
- 12) a) M. Ichikawa, T. Kawaguchi, K. Kobayashi, T. Miki, K. Furukawa, K. Koyama, Y. Taniguchi, *J. Mater. Chem.* **2006**, *16*, 221–225; b) M. Ichikawa, S. Fujimoto, Y. Miyazawa, T. Koyama, N. Yokoyama, T. Miki, Y. Taniguchi, *Org. Electron.* **2008**, *9*, 77–84; c) M. Uchida, T. Izumizawa, T. Nakano, S. Yamaguchi, K. Tamao, K. Furukawa, *Chem. Mater.* **2001**, *13*, 2680–2683.
- 13) Triazine-based materials: a) H. Inomata, K. Goushi, T. Masuko, T. Konno, T. Imai, H. Sasabe, J. J. Brown, C. Adachi, *Chem. Mater.* **2004**, *16*, 1285–1291; b) J. Pang, J. Tao, S. Freiberg, X. P. Yang, M. D'Ilorio, S. Wang, *J. Mater. Chem.* **2002**, *12*, 206–212; c) R. Fink, C. Frenz, M. Thelakkat, H. W. Schmidt, *Macromolecules* **1997**, *30*, 8177–8181.
- 14) For example: a) J. Chen, C. C. W. Law, J. W. Y. Lam, Y. Dong, S. M. F. Lo, I. D. Williams, D. Zhu, B. Z. Tang, *Chem. Mater.* **2003**, *15*, 1535–1546; b) G. Yu, S. Yin, Y. Liu, J. Chen, X. Xu, X. Sun, D. Ma, X. Zhan, Q. Peng, Z. Shuai, B. Tang, D. Zhu, W. Fang, Y. Luo, *J. Am. Chem. Soc.* **2005**, *127*, 6335–6346; c) S. H. Lee, B.-B. Jang, Z. H. Kafafi, *J. Am. Chem. Soc.* **2005**, *127*, 9071–9078.
- 15) a) M. A. Lampert, P. Mark, *Current Injection in Solids*, Academic Press, New York, **1970**; b) *Photoconductivity and Related Phenomena* (Eds.: J. Mort, D. M. Pai), Elsevier, New York, **1976**.
- 16) G. G. Malliaras, Y. Shen, D. H. Dunlap, H. Murata, Z. H. Kafafi, *Appl. Phys. Lett.* **2001**, *79*, 2582–2584.
- 17) *Gaussian 03*, Revision B.05, M. J. Frisch, G. W. Trucks, H. B. Schlegel, G. E. Scuseria, M. A. Robb, J. R. Cheeseman, J. A. Montgomery, Jr., T. Vreven, K. N. Kudin, J. C. Burant, J. M. Millam, S. S. Iyengar, J. Tomasi, V. Barone, B. Mennucci, M. Cossi, G. Scalmani, N. Rega, G. A. Petersson, H. Nakatsuji, M. Hada, M. Ehara, K. Toyota, R. Fukuda, J. Hasegawa, M. Ishida, T. Nakajima, Y. Honda, O. Kitao, H. Nakai, M. Klene, X. Li, J. E. Knox, H. P. Hratchian, J. B. Cross, C. Adamo, J. Jaramillo, R. Gomperts, R. E. Stratmann, O. Yazyev, A. J. Austin, R. Cammi, C. Pomelli, J. W. Ochterski, P. Y. Ayala, K. Morokuma, G. A. Voth, P. Salvador, J. J. Dannenberg, V. G. Zakrzewski, S. Dapprich, A. D. Daniels, M. C. Strain, O. Farkas, D. K. Malick, A. D. Rabuck, K. Raghavachari, J. B. Foresman, J. V. Ortiz, Q. Cui, A. G. Baboul, S. Clifford, J. Cioslowski, B. B. Stefanov, G. Liu, A. Liashenko, P. Piskorz, I. Komaromi, R. L. Martin, D. J. Fox, T. Keith, M. A. Al-Laham, C. Y. Peng, A. Nanayakkara, M. Challacombe, P. M. W. Gill, B. Johnson, W. Chen, M. W. Wong, C. Gonzalez, J. A. Pople, Gaussian, Inc., Pittsburgh, PA, **2003**.

Received: February 8, 2010

Published online: April 15, 2010